Self-Consistent-Field Analysis of the Micellization of Carboxy-Modified Poly(ethylene oxide)−poly(propylene oxide)−poly(ethylene oxide) Triblock Copolymers

Y. Lauw,* F. A. M. Leermakers, and M. A. Cohen Stuart

Laboratory of Physical Chemistry and Colloid Science, Wageningen University, Dreijenplein 6, Wageningen 6700 EK, The Netherlands

Received: July 11, 2005; In Final Form: October 25, 2005

The micellization properties of carboxy-modified Pluronics P85 (poly(ethylene oxide)−poly(propylene oxide)−poly(ethylene oxide) (PEO−PPO−PEO) triblock copolymers) are investigated by means of a molecularly realistic self-consistent-field theory. We consider the, so-called, carboxylic acid end-standing P85 (CAE-85) case where the carboxylic group is located at the end of both PEO parts and the carboxylic acid center-standing P85 (CAC-85) case where each of the carboxylic group presents between the PEO and PPO blocks. The micellization of these copolymers depends on the pH, the added electrolyte concentration φ_s, and the temperature. It is shown that the aggregation number (N_{agg}) decreases, whereas the critical micellization concentration (CMC) increases with pH. For the case of increasing φ_s, the N_{agg} increases and the CMC decreases. The critical micellization temperature (CMT) and cloud point temperature (CPT) increase with pH at low φ_s and decrease at increasing φ_s. The changing from CAE-85 to CAC-85 leads to increasing CMC and CMT, but lower CPT.

I. Introduction

Pluronic surfactants, also known as Poloxamer or Synperonic, are nonionic triblock copolymers with a general structure $(EO)_m(PO)_n(EO)_m$, where EO and PO represent an ethylene oxide and a propylene oxide group, respectively. The EO block with degree of polymerization m is the hydrophilic group and PO with length n is the hydrophobic part. Pluronics are widely used as detergents in pharmaceutical (drug delivery) and surface chemistry (wetting) applications. The micellization of this block copolymeric surfactant in aqueous solution has been studied widely, both experimentally and theoretically.[1−11] It is known that the micellization of Pluronic surfactants, or in general PEO-based surfactants, depends strongly on the temperature. In general, the critical micellization temperature (CMT) and cloud point temperature (CPT) define the temperature range over which a particular surfactant can be used.[12] Analogous to the critical micellization concentration (CMC), below the CMT, micellization does not occur, whereas above the CPT, the macroscopic phase separation is noticed.

The increase of temperature makes PEO-based surfactants more hydrophobic.[13,14] For the case of Pluronic surfactants, the increase in temperature causes an increase in the micellar dehydration since the effective interactions between the surfactants and water become less favorable. The rise in temperature also increases the aggregation number (N_{agg}) (size of the micelle) and reduces the CMC.[10,15,16] It is observed however that the hydrodynamic radius of a micelle is relatively independent of the temperature.[10,17] This is due to the compensating effect between the reduction of the corona swelling (because of the collapsing corona chains) and the increase of the aggregation number with increasing temperature.

The experimental phase diagram for Pluronic P85 in aqueous solution has been produced by Mortensen et al.[6,18] In such a phase diagram, information about the micellar shape and thermodynamic (colloidal) stability is collected as a function of the surfactant concentration and the temperature. The effect of salt on the micellization of Pluronic surfactants has also been documented by various authors.[19−24] In general, a sufficient increase in salt concentration decreases slightly the CMT and CPT.

In this article, we model the self-assembly of block copolymers composed of particular Pluronic surfactants P85, i.e., $(EO)_m(PO)_n(EO)_m$, where $m = 26$ and $n = 39$, which are chemically modified such that each molecule has two carboxylic groups.[25] By coupling the carboxylic groups to the *P*85 surfactant, a thermosensitive ionic block copolymer with pH-dependent charged groups is formed. Depending on the pH, the block copolymers as well as their corresponding micelles become charged. The micellization of ionic surfactants depends significantly on the amount of added electrolyte. As a result, the micellization of modified Pluronics can be adjusted by the pH, added electrolyte concentration φ_s, and temperature.

Micelles that exist beyond their corresponding CMC and CMT values can be found in various structures. The structure of a micelle is usually rationalized by the, so-called, packing parameter *P*. It is defined as the ratio of the volume of the tail (hydrophobic) group with the product of the head (hydrophilic) group area and the length of the tail group. The packing parameter value for spherical micelles is $P \leqslant 1/3$, for cylindrical micelles $1/3 < P \leqslant 1/2$ and planar bilayers $1/2 < P \leqslant 1$.[26] The packing parameter for the carboxy-modified P85 block copolymer depends undoubtedly on the pH, added electrolyte concentration and temperature. However, one needs a detailed molecular model to quantify these dependences. It is clear that for such a detailed model, the surfactant packing parameter is a possible intermediate quantity. In any case, results of a detailed molecular model may still be explained qualitatively by the notion of changes in the surfactant packing parameter. However, one may also bypass this parameter and focus directly on the micelles. Indeed, this range of physicochemical control parameters calls for a detail molecular modeling effort to guide the experimental work in characterizing this system. We apply the

10.1021/jp053795a CCC: $33.50
Published on Web 12/13/2005

self-consistent-field (SCF) lattice theory which was originally developed by Scheutjens and Fleer to model homopolymers adsorption at interfaces and modified further for self-assembly of ionic surfactants.[27−31] Here, we impose spherical geometry in the model such that only spherical micelles are considered. Under this geometrical constraint, we investigate the variation of micellar size as a function of the pH and the electrolyte concentration φ_s as a quantitative study of the change of the micellar packing parameter P (within the spherical regime) that corresponds to these governing variables.

Anticipating the experimental work on ionic thermoreversible block copolymer systems, we focus on two types of modifications of the P85 surfactants. They differ with respect to the position of the carboxylic group X in the block copolymers, i.e., X−$(EO)_{26}$−$(PO)_{39}$−$(EO)_{26}$−X and $(EO)_{26}$−X−$(PO)_{39}$−X−$(EO)_{26}$. They are named carboxylic acid end-standing P85 (CAE-85) and carboxylic acid center-standing P85 (CAC-85), respectively. The dissociation of carboxylic groups in CAE-85 and CAC-85 block copolymers in the micelles is expected to differ because of the different average position of the X group in the micelle with concomitant influences on the electrostatics.

The remainder of this paper is as follows: We start by briefly reviewing the thermodynamics of small systems that are used to interpret the micellar behavior as found in the Scheutjens−Fleer self-consistent-field (SF−SCF) calculation. The SF−SCF model is discussed in more detail before the model parameters are presented. It is followed by results and discussions. The paper is closed by concluding remarks.

II. Thermodynamics of a Small System

The thermodynamical background of self-assembly has a solid foundation in the thermodynamics of small systems initiated by Hill.[32] It was elaborated further for the case of surfactant micellization by Hall and Pethica.[33] The SF-SCF model is a convenient (statistical) thermodynamical framework that is ideally suited for such small system analysis. This method has been used previously for surfactant (copolymer) systems. Here, we review the important steps and extend the method to deal with micellization of the ionic block copolymer with charge annealing groups.

In the classical thermodynamics, according to Gibbs,[34] in a macroscopic system consisting of c components, the change of internal energy dU due to the change of entropy dS, volume of the system dV, and the total number of molecules of the ith component dN_i, at temperature T, pressure p, and chemical potential of all components μ_i, is given by

$$\mathrm{d}U = T\,\mathrm{d}S - p\,\mathrm{d}V + \sum_i^c \mu_i\,\mathrm{d}N_i \tag{1}$$

In the case of micellization, this expression is extended by introducing two conjugated quantities, i.e., the subdivision potential $\mathcal{E}$ and the number of micelles $\mathcal{N}$,[16,17] such that

$$\mathrm{d}U = T\,\mathrm{d}S - p\,\mathrm{d}V + \sum_i^c \mu_i\,\mathrm{d}N_i + \mathcal{E}\,\mathrm{d}\mathcal{N} \tag{2}$$

Therefore, the change of the Helmholtz energy dF, where $F = U - TS$, can be expressed as

$$\mathrm{d}F = -S\,\mathrm{d}T - p\,\mathrm{d}V + \sum_i^c \mu_i\,\mathrm{d}N_i + \mathcal{E}\,\mathrm{d}\mathcal{N} \tag{3}$$

where the equilibrium and the stability conditions lead to two constraints

$$\left.\frac{\partial F}{\partial \mathrm{N}}\right|_{T,V,\{N_i\}} = \mathcal{E} = 0 \tag{4}$$

$$\left.\frac{\partial^2 F}{\partial \mathcal{N}^2}\right|_{T,V,\{N_i\}} = \left.\frac{\partial \mathcal{E}}{\partial \mathcal{N}}\right|_{T,V,\{N_i\}} > 0 \tag{5}$$

Equation 4 ensures that at equilibrium, the macroscopic thermodynamics for a homogeneous phase, as expressed in eq 1, is conserved. Equation 5 assures the stability of the micellization. Furthermore, under isothermic condition, based on eq 3, one obtains

$$F = -pV + \sum_i^c \mu_i N_i + \mathcal{E}\mathcal{N} \tag{6}$$

or equivalently

$$F + pV - \sum_i^c \mu_i N_i = \mathcal{E}\mathcal{N} \tag{7}$$

The complete subdivision potential $\mathcal{E}$ cannot be computed by SCF type of modeling. The reason is that in the numerical procedure, one considers one micelle in the center of the coordinate system. Instead, the grand potential per micelle Ω is obtained and interpreted as the translationally restricted $\mathcal{E}$. Therefore, an extra entropic term S_{extra}, which is coupled to degrees of freedom at the level of the whole micellar object and that is ignored by the SCF method, has to be added to regain the complete subdivision potential

$$\Omega - TS_{\mathrm{extra}} = \mathcal{E} \tag{8}$$

As already referred to in the Introduction, in the SCF system (one micelle is in the center of the coordinate system), equivalent to eq 5, the relevant stability constraint is reformulated as

$$\left.\frac{\partial \Omega}{\partial \mathcal{N}}\right|_{T,V,\{N_i\}} > 0 \tag{9}$$

Since in a closed system with constant number of surfactants (copolymers) the number of micelles $\mathcal{N}$ is reduced upon increasing aggregation number N_{agg}, the stability condition can be rewritten as

$$\left.\frac{\partial \Omega}{\partial N_{\mathrm{agg}}}\right|_{T,V,\{N_i\}} < 0 \tag{10}$$

In general, the micelles will not all have the same size. Although the size distribution can be accounted for, in the following we will ignore this level of complexity and assume all micelles to be of the same size.

If stable monodisperse micelles exist for a particular chemical potential of copolymers, the extra entropic term S_{extra} is just the translational entropy S_{trans} of a micelle, i.e., $S_{\mathrm{trans}} \simeq -k_{\mathrm{B}} \ln \varphi_{\mathrm{m}}$, where φ_{m} is the volume fraction occupied by a micelle. As the system is macroscopically homogeneous and each small system has a single micelle, the volume fraction of the micelles is given by the ratio of the intrinsic volume of the micelle v_{m} and the volume of the small system $v = V/N$. The intrinsic

volume of the micelle can be estimated by

$$v_m \simeq \theta_p^{exc} a^3 \tag{11}$$

where θ_p^{exc} is the total excess number of copolymer segments in the micelle, i.e., the excess number of copolymers multiplied by total number of segments of each copolymer. The parameter a is the characteristic size of one segment. Therefore, a^3 is the unit volume of each segment (further discussion about the discretization and numerical scheme can be found in the next section). By use of expression 11, the micellar volume fraction can be written as

$$\varphi_m = \frac{\theta_p^{exc}}{v} a^3 = \frac{\theta_p^{exc} \mathcal{N}}{V} a^3 \tag{12}$$

Obviously, the Ansatz $S_{trans} \simeq -k_B \ln \varphi_m$ only applies when the micelle is in a very dilute solution such that there are no steric and electrostatic interactions between micelles (for the case of ionic micelle). In a dilute solution and at equilibrium, the micelle volume fraction φ_m is thus directly related to the grand potential

$$\varphi_m = e^{-\Omega/k_B T} \tag{13}$$

As mentioned earlier, within the SCF model, one obtains the most likely micellar size and small fluctuations around this size are ignored. In eq 13, the entropy associated with the fluctuations in size is not included, whereas it should be accounted for in a more complete model. Here, we restrict ourselves to the first-order effects.

III. Self-Consistent-Field Theory of a Weakly Charged System

The self-consistent-field (SCF) model of spatially inhomogeneous assemblies of chain molecules with charge annealing groups is based on the, so-called, multiple-state approximation initiated by Bjorling et al.[35] The model was elaborated and applied to an annealed polyelectrolyte system by Israëls and Van Male.[36,37] In short, this model deals with the possibility of a particular segment of a molecule to exist in different internal states. For example, a carboxylic group can exist as a negatively charged or as a neutral group, depending on its protonation. In this article, we use this model to describe the two charged carboxylic groups within the block copolymers as well as for self-dissociation of water molecules.

To determine the statistical weight of various conformations of molecules, these molecules are considered to be composed of segments. A sequence of segments defines the architecture of a molecule. Space is discretized by using a lattice. Each segment just fits one lattice site with characteristic size a. All distances are normalized to dimensionless quantities by this characteristic size. It is essential to know that in this lattice system there exist layers of lattice sites in which the density of molecular components is assumed to be homogeneous and that gradients in density can develop between different layers.

Since we describe spherosymmetric objects, we use a spherical coordinate system. The radial direction is denoted by the layer number r. Within a mean-field approximation, it is sufficient to specify the density of a segment type for each layer r. Therefore, there is only one governing variable, which is the radial layer number r that runs from 0 to M; $r = 0$ is the center of the spherical coordinate system. M is taken large enough to ensure that at least at the last layer the bulk phase properties exist.

As our SF-SCF model requires us to work in terms of discretize (dimensionless) variable quantities at particular layer r, we refer these quantities as *operative* variables in contrast to *experimental* variables which denote the standard variables that are used in reality. Throughout this article, except for the volume fraction notation, we use the tilde symbol for the operative variables to distinguish them from the standard experimental variables. In the next section, we explain in more detail how both type of variables are connected.

The statistical weight of the free segments of type A in internal state j at layer r is expressed as a segment-weighting factor $G_{A_j}(r)$ which is defined as

$$G_{A_j}(r) = \begin{Bmatrix} \exp\left\{\dfrac{-u_{A_j}(r)}{k_B T}\right\}, & 0 < r < r_{bulk} \\ 1, & r \geq r_{bulk} \end{Bmatrix} \tag{14}$$

where $u_{A_j}(r)$ is the potential energy of segment A in state j at layer r, k_B is the Boltzmann constant, T is the absolute temperature, and r_{bulk} is the layer number in the bulk, i.e., $r_{bulk} \geqslant M$. In the case of a weakly charged group/segment, we consider states that differ in their valence. On the basis of the multiple-state model,[35] the overall statistical weight of segments of type A, $G_A(r)$, is built up from the weighted sum over state-dependent segment-weighting factors $G_{A_j}(r)$[38]

$$G_A(r) = \sum_j \alpha_{A_j}^b G_{A_j}(r) \tag{15}$$

where α_{Aj}^b is the fraction of segments A in state j in the bulk phase.

In this article, we consider that the carboxylic groups X in the block copolymers CAE-85 and CAC-85 can exist in two states, X_1 and X_2. Segment X_1 represents the uncharged state COOH, whereas X_2 stands for the charged state COO^-. In aqueous solution, the two states are coupled through the dissociation equation

$$COOH + H_2O \rightleftharpoons COO^- + H_3O^+ \tag{16}$$

$$\tilde{K}_a = \frac{\varphi_{COO^-} \cdot \varphi_{H_3O^+}}{\varphi_{COOH} \cdot \varphi_{H_2O}}$$

where φ_i denotes the volume fraction of segment i. The water equilibrium is given by

$$2H_2O \rightleftharpoons H_3O^+ + OH^- \tag{17}$$

$$\tilde{K}_w = \frac{\varphi_{H_3O^+} \cdot \varphi_{OH^-}}{(\varphi_{H_2O})^2}$$

Here, water has three states, H_2O, H_3O^+, and OH^-, denoted by W_1, W_2, and W_3, respectively. The $\tilde{K}_a$ is the corresponding operative dissociation constant of the segment type X and $\tilde{K}_w$ is that of water. The fraction of segments COO^- in the bulk phase $\alpha_{COO^-}^b$ is the ratio between the bulk volume fraction $\varphi_{COO^-}^b$ with the total bulk volume fraction of carboxylic groups

$$\alpha_{COO^-}^b = \frac{\varphi_{COO^-}^b}{\varphi_{COO^-}^b + \varphi_{COOH}^b} \tag{18}$$

The full protonation of the segment X, i.e., $\alpha^{b}_{COO^-} = 0$, happens at low pH. At high pH, the X group is completely deprotonated ($\alpha^{b}_{COO^-} = 1$).[39,40] Combination of eqs 16 and 18 in the bulk solution leads to

$$p\tilde{K}_a + p\tilde{H}_2O = p\tilde{H} - \log \frac{\alpha^{b}_{COO^-}}{1 - \alpha^{b}_{COO^-}} \tag{19}$$

where $p\tilde{K}_a = -\log \tilde{K}_a$, $p\tilde{H}_2O = -\log(\varphi_{H_2O})$, and $p\tilde{H} = -\log(\varphi_{H_3O^+})$.

By using the value of $p\tilde{K}_a$ at a certain proton concentration in the bulk as an input parameter, all values of α^{b}_{Aj} can be found using eqs 18 and 19. The fraction of segments A in state j at layer r is found from[36]

$$\alpha_{A_j}(r) = \frac{\alpha^{b}_{A_j} G_{A_j}(r)}{G_A(r)} \tag{20}$$

In eq 14, the potential $u_{A_j}(r)$, also known as the self-consistent potential, consists of two classical terms, i.e., a Lagrange field and a contribution due to contact energy. The presence of charges in the system leads to two extra electrostatic contributions in the self-consistent potential[37]

$$u_{A_j}(r) = u'(r) + k_B T \sum_B \sum_k \chi_{A_j B_k}(\langle \varphi_{B_k}(r)\rangle - \varphi^{b}_{B_k}) + e\upsilon_{A_j}\Psi(r) - \frac{1}{2}\epsilon_0(\epsilon_{r,A_j}(r) - 1)P(r) \tag{21}$$

Here, $u'(r)$ is the potential energy required to guarantee that in each layer all lattice sites are occupied by segments (incompressibility constraint). The second term of the equation describes the potential due to the interactions between segments in the system. The Flory−Huggins interaction parameter between segment type A in the state j and B in the state k is denoted as $\chi_{A_jB_k}$; $\varphi_{B_k}(r)$ is the volume fraction of segment type B in the state k at layer r. The angular brackets indicate the averaging over the neighboring layers of r. The notation $\varphi^{b}_{B_k}$ refers to the volume fraction of segment type B in the state k in the bulk phase. The third term of the equation is the electrostatic contribution due to the presence of the free charges; e is the elementary charge, υ_{A_j} the valence of segment A in state j, and $\Psi(r)$ the electrostatic potential in layer r. The fourth term is the electrostatic contribution due to the presence of the segment polarization. Here, ϵ_0 is the dielectric permittivity in a vacuum, $\epsilon_{r,A_j}(r)$ the relative dielectric constant of segment A in state j at layer r, and $P(r)$ is the average of the square of the electrostatic potential with respect to the two halves of adjacent layers r.

In the numerical scheme, the electrostatic potential $\Psi(r)$ is obtained from solving a discrete form of the Poisson equation. For the spherical coordinate system, it is given by

$$\epsilon_0 \frac{1}{r^2}\frac{d}{dr}\left(r^2\epsilon_r(r)\frac{d\Psi(r)}{dr}\right) = -\rho(r) \tag{22}$$

$$\forall r \in [0, M]$$

where $\rho(r)$ and $\epsilon_r(r)$ are the charge distribution and the total relative dielectric permittivity of layer r, respectively. They are obtained by the summation of each charge and relative dielectric permittivity over all segment in their possible states, i.e.

$$\rho(r) = \frac{\sum_A \sum_j e\upsilon_{A_j}\varphi_{A_j}(r)L(r)}{S(r)} \tag{23}$$

$$\epsilon_r(r) = \sum_A \sum_j \epsilon_{r,A_j}(r)\varphi_{A_j}(r) \tag{24}$$

where $L(r)$ is the total number of lattice sites in layer r and $S(r)$ is the contact area between layer r and $(r + 1)$. In the spherical lattice, $S(r) = 4\pi r^2$ and $L(r) = 4\pi(r^2 - r + {}^1/_3)$.

The particular solution of eq 22 is found by applying a boundary condition that comes from the electroneutrality condition in the system

$$\left.\frac{d\Psi(r)}{dr}\right|_{r=M} = 0 \tag{25}$$

The term $\langle\varphi_{B_k}(r)\rangle$ in eq 21 is obtained by averaging the volume fraction $\varphi_{B_k}(r)$ over adjacent layers

$$\langle\varphi_{B_k}(r)\rangle = \lambda_{-1}(r)\varphi_{B_k}(r-1) + \lambda_0(r)\varphi_{B_k}(r) + \lambda_1(r)\varphi_{B_k}(r+1) \tag{26}$$

where $\lambda_{-1}(r)$, $\lambda_0(r)$, and $\lambda_1(r)$ are known as bond-weighting factors. They depend on the coordinate system that is used and are given by[41]

$$\lambda_{-1}(r) = \lambda\frac{S(r-1)}{L(r)} \tag{27}$$

$$\lambda_1(r) = \lambda\frac{S(r)}{L(r)} \tag{28}$$

$$\lambda_0(r) = 1 - \lambda_{-1}(r) - \lambda_1(r) \tag{29}$$

The quantity λ is the one-dimensional bond-weighting factor. It is easily verified that eqs 27−29 are consistent with respect to the internal balance $L(r + 1)\lambda_{-1}(r + 1) = L(r)\lambda_1(r)$.

The segment-weighting factor $G_A(r)$, which depends on the segment type, can be generalized to a similar quantity that depends on the type of molecule i and segment ranking number s in the molecule. By introducing the chain architecture operator $\delta^{A}_{i,s}$ with property $\delta^{A}_{i,s} = 1$ when segment s of molecule i is of type A and zero otherwise, one can write

$$G_i(r,s) = \sum_A G_A(r)\delta^{A}_{i,s} \tag{30}$$

The segment-weighting factors $G_i(r,s)$ are used to obtain the chain segment-weighting factor $G_i(r, s|1)$ for segment s of molecule i at layer r connected by $s - 1$ segments to segment $s = 1$. This is performed by using a Markov approximation which leads to the propagator equation

$$G_i(r, s|1) = \begin{Bmatrix} G_i(r,1) & , s = 1 \\ \langle G_i(r, s-1|1)\rangle G_i(r,s) & , s > 1 \end{Bmatrix} \tag{31}$$

The average chain segment weighting factor $\langle G_i(r, s - 1|1)\rangle$, analogous to the average volume fraction, is weighted by the spatial (lattice geometry) dependent bond-weighting factors

$$\langle G_i(r, s-1|1)\rangle = \lambda_{-1}(r)G_i(r-1, s-1|1) + \lambda_0(r)G_i(r, s-1|1) + \lambda_1(r)G_i(r+1, s-1|1) \tag{32}$$

The complementary chain segment weighting factor $G_i(r, s|N)$, i.e., the quantity that is proportional to the probability of finding a chain fragment from the last segment N_i to s such that segment s of molecule i is at r, is evaluated using the complementary equations (31) and (32). When all segment weighting factors are known, the volume fraction of segment s of molecule i is obtained from the composition law

$$\varphi_i(r,s) = C_i \frac{G_i(r, s|1)G_i(r, s|N)}{G_i(r, s)} \tag{33}$$

where C_i is a normalization factor which, for a grand canonical ensemble (φ_i^b fixed), is equal to φ_i^b/N_i. Alternatively, C_i depends on the number of molecules n_i of type i in the system such that $C_i = n_i/G_i(1|N)$, where $G_i(1|N) = \sum_r L(r)G_i(r, 1|N)$. Analogous to the segment-weighting factor, the volume fraction $\varphi_A(r)$ of the segment type A is obtained from its more general form $\varphi_i(r,s)$ that depends on the type of molecule i and segment ranking number s in the molecule

$$\varphi_A(r) = \sum_i \sum_s \varphi_i(r,s)\delta_{i,s}^A \tag{34}$$

For a given initial set of volume fractions $\varphi_A(r)$, the potential energy for each segment or segment with different state is found through eq 21. An important condition that has to be satisfied is $\sum_A\sum_j\varphi_{A_j}(r) = 1$ for all layers r. This is also known as the packing (incompressibility) constraint which determines the values of $u'(r)$. The segment-weighting factor for each molecule and each segment ranking number in a chain is calculated with eq 30 via eqs 14 and 15. Finally, the volume fraction of each segment type can be recalculated by using eqs 33 and 34. The set of equations is thus closed, and an iterative procedure is applied until all potentials $u_{A_j}(r)$ and segment volume fractions $\varphi_{A_j}(r)$ are self-consistent. Once this solution is known, the partition function can be considered to be optimized and the grand potential Ω can be evaluated. The grand potential can be written as[42]

$$\frac{\Omega}{k_BT} = -\sum_r L(r)\Pi(r) \tag{35}$$

where $-\Pi(r)$ is known as the dimensionless grand potential density

$$\Pi(r) = \sum_A\sum_j \varphi_{A_j}(r)\frac{u_{A_j}(r)}{k_BT} + \sum_i \frac{\varphi_i(r) - \varphi_i^b}{N_i} - \frac{1}{2}\sum_A\sum_j\sum_B\sum_k \chi_{A_jB_k}\{\varphi_{A_j}(r)(\langle\varphi_{B_k}(r)\rangle - \varphi_{B_k}^b) - \varphi_{A_j}^b(\varphi_{B_k}(r) - \varphi_{B_k}^b)\} - \frac{1}{2}\sum_A\sum_j ev_{A_j}\varphi_{A_j}(r)\frac{\Psi(r)}{k_BT} \tag{36}$$

where $\varphi_i(r) = \sum_s\varphi_i(r,s)$ gives the overall density of molecule i at layer r.

Another important thermodynamic quantity is the chemical potential $\mu_{i,t}$ of molecule i in state t. A molecular state t is defined by the states of each of its segments. Furthermore, it is sufficient only to specify the chemical potential for a particular state t since all states are in mutual equilibrium. The chemical potential $\mu_{i,t}$ is defined as

$$\mu_{i,t} = \left.\frac{\partial F}{\partial n_{i,t}}\right|_{\{n_{j\neq i,u\neq t}\}} \tag{37}$$

where $n_{i,t}$ is the number of molecules i at state t. By applying eq 37 to the free energy of the homogeneous bulk solution, one finds[37]

$$\frac{\mu_{i,t}}{k_BT} = \ln\varphi_{i,t}^b + 1 - N_i\sum_j\frac{\varphi_j^b}{N_j} + \sum_A\sum_j\sum_B\sum_k N_{i,t,A_j}\chi_{A_jB_k}\varphi_{B_k}^b - \frac{1}{2}N_i\sum_A\sum_j\sum_B\sum_k\varphi_{A_j}^b\chi_{A_jB_k}\varphi_{B_k}^b + \sum_A\sum_j N_{i,t,A_j}\ln\alpha_{A_j}^b \tag{38}$$

where $\varphi_{i,t}^b$ is the volume fraction of molecule i at the state t in the bulk and N_{i,t,A_j} is the number of segments A in the state j at molecule i of the state t. The last term in the right-hand side is the contribution of chemical potential from the segments in different states in the equilibrium. It is important to be noted that there is no effect of charges on the chemical potential since only bulk properties are used and there is no electrostatic potential in the bulk.

IV. Model Parameters

There are four types of input parameters that have to be predefined before starting the SCF calculation. The first set of input parameters determines the architecture of the chains, the total number of molecules in the system, and the possible internal states of each segment. The second set is the Flory−Huggins interaction parameters between all segments, the third is the dissociation constants and electrostatic properties of each segment in the internal states level, and the fourth contains details of the lattice coordinate system.

In the calculations, we use two types of modified Pluronic CAE-85 and CAC-85. The sequence of their segments are as follows: $X(C_2O)_{26}(C_2C^{br}O)_{39}(C_2O)_{26}X$ and $(C_2O)_{26}$ X-$(C_2C^{br}O)_{39}X(C_2O)_{26}$, respectively. The carboxylic group is indicated as X. It exists as either a neutral segment or a negatively charged ion. C refers to the CH_2 group, O resembles the oxygen group, and C^{br} as a CH_3 group (which in PO is a side group but in our model is located in the linear chain). Water is modeled as a monomer and it is weakly dissociated which depends on the pH. As an electrolyte, 1:1 electrolyte is used. It is important to note that the electrolyte concentration φ_s is expressed in a dimensionless unit, thus as an operative variable. To convert this (or other monomeric volume fraction) to molar value, a conversion factor of 55.4 M is used, following the concentration value given from the monomeric solvent. For example, $\varphi_s = 10^{-5}$ corresponds to 5.5×10^{-4} M salt concentration. In this article, the notation φ_s denotes the volume fraction (linearly proportional to the concentration) of the added electrolyte in the bulk; i.e., the bulk notation is omitted.

Generally in the SF-SCF calculation, the operative variables are used. As already shown above, these variables are translated into experimetal variables (and vice versa) by using a conversion factor of 55.4 M. Another example is that the experimental pH = 7 is equivalent with the operational $p\tilde{H} = -\log(10^{-7}/55.4) \approx 8.74$. In this article, except for the added electrolyte volume fraction φ_s, the experimental variables are used in describing the results. The experimental variables are derived by converting

TABLE 1: List of the Flory−Huggins Interaction Parameters Used in the Model

χ	X	C	O	C^{br}	W	s
X	0	1.6	−0.7	2.3	0	0
C	1.6	0	1	0.6	1.6	1.6
O	−0.7	1	0	1.6	−0.7	−0.7
C^{br}	2.3	0.6	1.6	0	2.3	2.3
W	0	1.6	−0.7	2.3	0	0
s	0	1.6	−0.7	2.3	0	0

the operative variables in the same way as already described in the examples.

In general, a Flory−Huggins interaction parameter consists of an enthalpic and an entropic contribution. The dimensionless interaction parameter can be split up as $\chi_{ij} = A_{ij} - B_{ij}/T$, where A_{ij} is the entropic and B_{ij} the enthalpic part. To predict the temperature dependence of the micellization, it is thus necessary to specify all A_{ij} and B_{ij} values. However, most of these parameters are largely unknown. Therefore, we implement a highly simplified approach which is motivated by the following arguments. It is known that at room temperature the solubility of apolar molecules such as alkanes in water are not a strong function of the temperature.[13] This implies an insignificant enthalpic contribution in the corresponding χ parameter value ($B_{CW} = B_{C^{br}W} \approx 0$). The self-assembly of Pluronics does however depend strongly on the temperature. This suggests a strong temperature-dependent hydration of the O groups by water molecules, thus to a temperature-dependent χ_{OW}.[43,44] The simplest model that gives the trends in the micellization of P85 and its carboxy-modified variants is by implementing the Ansatz that χ_{OW} is the only parameter that is a function of the temperature. Here, we use a more negative χ_{OW} value for low temperature and a less negative one for higher temperature.

In a previous publication by De Bruijn et al.,[44] several χ parameter sets for the modeling of Pluronic self-assembly were used. These parameter sets were not optimized yet because there are no exact experimental data available (since the Pluronics are polydisperse). Therefore, we consider the parameters of De Bruijn as rough indications. Nevertheless, we closely follow the χ parameters from the dimeric water model of De Bruijn. Since the water dissociation and the charge regulation of the carboxylic groups require a monomeric water component, we have modified the parameter set of De Bruijn with respect of the hydrocarbon−water interaction. Furthermore, the χ parameters for the monovalent salt *s* and carboxylic groups X follow the values of the water molecule for simplicity. The hydrophobicity of the PO block is reflected in a relatively high value of $\chi_{C^{br}W}$ compared with χ_{CW}. The full set of 12 χ parameters that are used in the model is listed in Table 1. We consider that the chosen χ parameters are reasonable, albeit not necessarily the most optimal ones.

The carboxylic group X dissociates with corresponding operational dissociation constant $p\tilde{K}_a = 6$, i.e., $pK_a = 4.25$.[45] It can exist in two possible states, with or without charge, with the valence value $\upsilon_{COO^-} = -1$ and $\upsilon_{COOH} = 0$, respectively. The relative permittivity ϵ_r of this group is set to be equal to 10. The other components in the Pluronic compound have zero valence. Each salt ion of 1:1 electrolyte is modeled as a monomer with valence $\upsilon_{s^+} = 1$ and $\upsilon_{s^-} = -1$. The relative permittivities for both ions are set equal to 10. Water is modeled as a monomer with $pK_w = 14$ ($p\tilde{K}_w = 17.5$). It exists in three possible states with corresponding valence $\upsilon_{OH^-} = -1$, $\upsilon_{H_2O} = 0$, and $\upsilon_{H_3O^+} = 1$. The relative permittivity of water is equal to 80. In the model, the operative $p\tilde{H} = -\log(\alpha^b_{H_3O^+} \cdot \varphi^b_W)$ is used, where $\alpha^b_{H_3O^+}$ is the degree of dissociation of proton in the bulk solution and φ^b_W is the volume fraction of the water also in the bulk. Again, the $p\tilde{H}$ corresponds to the experimental pH by using the conversion factor 55.4 M such that $p\tilde{H} = pH + \log 55.4$.

A spherical coordinate system is imposed in all calculations. The minimum total number of lattice layers $M = 150$ ensures that the bulk properties are attained at layer $r \approx M$ (where $r = 0$ is the center of the micelle). In all cases, the value of M is such that it exceeds the Debye length considerably, which causes the electrostatic potential to vanish at the system boundary. The one-dimensional bond-weighting factor λ in all calculations is set equal to $^1/_3$ and the characteristic dimension of a lattice site a is equal to 0.3 nm.

V. Results and Discussions

In the following, the micellization properties such as the aggregation number, the micellar size and CMC are shown to depend on the pH, salt concentration, temperature, and the position of carboxylic group in the modified Pluronic block copolymer. This section is composed of four parts. The first part contains a case study based on a system for particular physicochemical conditions, i.e., for block copolymer CAE-85 at pH = 7 and salt concentration $\varphi_s = 10^{-3}$ at room temperature which is for $\chi_{OW} = -0.7$. In the second part, the φ_s and pH dependences on the micellization are shown, followed in the third part by the effects of varying temperature (variation of χ_{OW}). Finally, the effects of the position of carboxylic groups in the modified Pluronic block copolymer on the micellization are presented.

A. Case Study: (CAE-85, pH = 7, $\varphi_s = 10^{-3}$). In this subsection, a case study is presented to illustrate results of SF-SCF calculations on the self-assembly of CAE-85 at pH = 7 and added electrolyte concentration $\varphi_s = 10^{-3}$. At this pH, most of the carboxylic groups of CAE-85 are almost fully charged. The degree of dissociation of this group in the bulk solution $\alpha^b_{COO^-}$ increases with pH as can be seen in Figure 1a, following exactly the predefined pK_a value. The radial profile of the degree of dissociation α_{COO^-} is depicted in Figure 1b. Here, $r = 0$ is the center of the micelle. It can be seen that α_{COO^-} in the micellar region slightly deviates from the bulk value ($\alpha^b_{COO^-} \approx 0.998$). The two minima in the curve correspond to the accumulation of carboxylic groups in these positions. This, as will be shown later, occurs at the so-called corona−solution interface. The local suppression of the carboxyl dissociation in this region is caused by the unfavorable local electrostatic potential (cf. Figure 2c).

In Figure 2a, the thermodynamic properties, such as translationally restricted grand potential Ω and chemical potential μ_p of CAE-85, are presented as a function of the aggregation number N_{agg}. At $N_{agg} \approx 26$, as indicated by the first pair of dots, the thermodynamical condition for stability of the micelles is fulfilled for the first time. This value corresponds to the theoretical CMC where the chemical potential of the copolymer reaches its lowest value. As the aggregation number increases, the Ω decreases and, correspondingly, μ_p increases. Eventually, at $N_{agg} \approx 78$, the grand potential reaches the value $\Omega = 0$. For $N_{agg} > 78$, the spherical micelles are too large such that other geometrical structures such as cylindrical micelles typically become relevant. The remainder of the results of Figure 2b−d are based on the system where the restricted grand potential $\Omega = 10 k_B T$.

The volume fraction profiles of PO and EO groups, φ_{PO} and φ_{EO}, in the radial direction r are depicted in Figure 2b. The region where the hydrophobic groups PPO are mostly located is known as the core. At this region ($r \lesssim 16$), $\varphi_{PO} \approx 0.6$. The

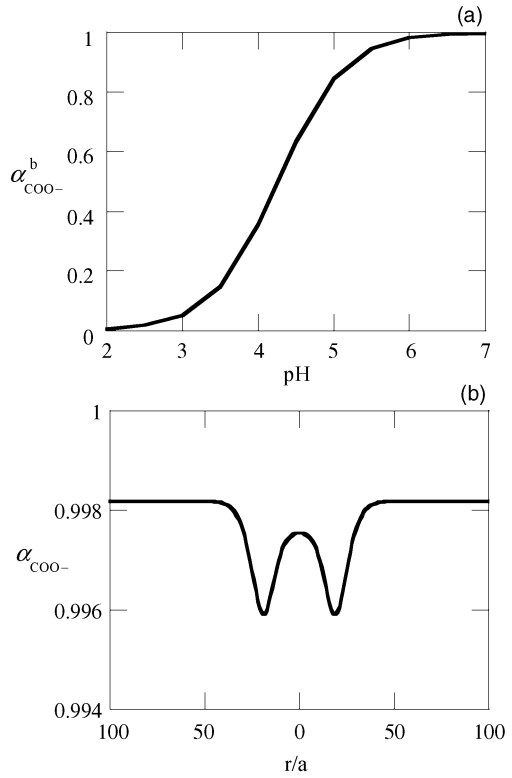

Figure 1. (a) Degree of dissociation in the bulk solution $\alpha^{b}_{COO^-}$ of carboxylic groups in block copolymers CAE-85 as a function of pH. (b) Radial profile of degree of dissociation α_{COO^-} of a micelle composed of CAE-85 block copolymers for conditions pH = 7 and $\varphi_s = 10^{-3}$. The micelle has a grand potential $\Omega = 10k_BT$.

hydrophilic PEO groups can be found mostly in the region which is called corona. It is located between the core and the bulk solution, i.e., at $16 \lesssim r \lesssim 20$. The peak of φ_{EO} lies just outside the core. The micellar size is discussed in more detail in the next section (cf. Figure 7c,d).

The radial profiles for the electrostatic potential, $\Psi(r)$, and the corresponding overall charge, $q(r)$, are shown in Figure 2c. As the dissociation of carboxylic groups causes the finite electrostatic potential in the micelle, the $\Psi(r)$ is negative throughout the whole system. The electroneutrality of the overall system implies that there are both positive and negative values in the charge profile. From these two profiles in Figure 2c, the bulk solution is found for $r > 50$, as in this part of the system both the electrostatic potential and the overall charge are zero. This proves that the system size M is sufficient to ensure that the bulk solution is attained. Indeed, the Debye length for this system is about 5 lattice units which is significantly smaller than the distance between the outer corona region ($r \approx 20$) to the system boundary ($r = M = 150$). A net positive charge occurs in the diffuse layer just outside the corona, i.e., at the corona−solution interface, as well as around the core−corona region. Here some counterions penetrate and accumulate. In the corona, the net negative charge is obtained as a result of the dissociation of the carboxylic groups. A diffuse double layer is formed by the accumulation of the counterions (the added electrolyte cations s^+) around and outside corona region (Figure 2d). As expected, the electrostatic potential drops exponentially following the Debye−Huckel behavior (low potentials). Moreover, due to the low dielectric permittivity in the core region, the total charge density in this region is relatively small and the electrostatic potential in the core−corona region also decreases gradually toward the center of the micelle, yet it does not reach the value zero.

A characteristic property for the formation of micelles is the distribution of copolymers in micellar and unimeric forms. At very low copolymers concentration, only unimers exist, whereas at high concentration, copolymers are mainly found in micelles. A plot showing the abrupt change of the total value φ_p of the volume fraction of the block copolymer CAE-85 in the system as a function of that in the bulk (φ^{b}_{p}) is depicted in Figure 3. In all cases, the total volume fraction of copolymers is the sum of those in micelles and in the bulk solution as unimers, i.e., $\varphi_p = \varphi_m + \varphi^{b}_{p}$ where φ_m is the volume fraction of block copolymer in the micellar form (eq 13). By locating the kink in the curve, the practical *CMC* value is obtained as indicated in the figure. In the region where $\varphi_p(\varphi^{b}_{p})$ is strongly curved, the micelle size changes rapidly.

For low molecular weight surfactants, a similar curve is found, where the kink corresponds closely to the theoretical and experimental CMC. Close inspection of Figure 3 shows that for the polymeric surfactant based on P85, the kink occurs at extremely low volume fraction of micelles φ_m. Indeed, there exists no technique that can detect such low concentration of surfactants. This means that any experimentally determined CMC will differ significantly from the theoretical one and the kink in Figure 3 is not a convenient measure for the experimental CMC. To select the typical results for the present system as a function of various physicochemical parameters, it is necessary to focus on a relevant micellar system which is close to an experimentally observable case. We choose micelles that have a given translationally restricted grand potential of $\Omega = 10k_BT$ for this purpose. As expressed in eq 13, the corresponding micellar volume fraction is $\varphi_m = e^{-10} \approx 4.5 \times 10^{-5}$. This micellar concentration is considered to be notably present in the solution (e.g., by the light scattering technique). Although the choice is quite arbitrary, very similar results are obtained for other values on Ω. The results are therefore quite generic.

B. Salt Concentration and pH Dependence. In this subsection, there are three properties that are selected: the aggregation number N_{agg}, the CMC, and micellar size. The dependences on the amount of added salt φ_s and the pH are preceded by the discussion on the dissociation of the carboxylic group.

The local degree of dissociation α_{COO^-} of the carboxylic group in the CAE-85 micelle depends on the local electrostatic potential which is affected by salt as shown in Figure 4a. The radial profile of α_{COO^-} is in the range of $\varphi_s = 10^{-5}$ to 10^{-2} at pH = 4.5 (approximately the pK_a value). This profile follows the electrostatic potential. With increase of φ_s, the electrostatic potential is screened and allows further dissociation of weakly charged group toward the bulk value. A high value of the electrostatic potential leads to an increasing amount of counterions and subsequently higher screening of the potential. In the core region, a finite value of the electrostatic potential leads to a significant value for the degree of dissociation. However, there are only few carboxylic groups in the core.

In Figure 4b, the radial profiles of α_{COO^-} at $\varphi_s = 10^{-3}$ for pH = 3.5, 4, 4.5, 5, and 5.5 are depicted. It is obvious to see that the higher the pH, the higher is the local degree of dissociation. In the micellar region, for the case of pH < pK_a, i.e., at pH = 3.5 and 4, the electrostatic potential remains low since only few groups dissociate. At pH = 5.5 > pK_a, the electrostatic potential is relatively high at the corona−solution interface. Yet, since it is screened, the electrostatic potential has relatively little effect on the corresponding α_{COO^-} profile. At pH close to pK_a, the local variations in the degree of dissociation is the highest. Here, the electrostatic potential significantly suppresses the dissociation.

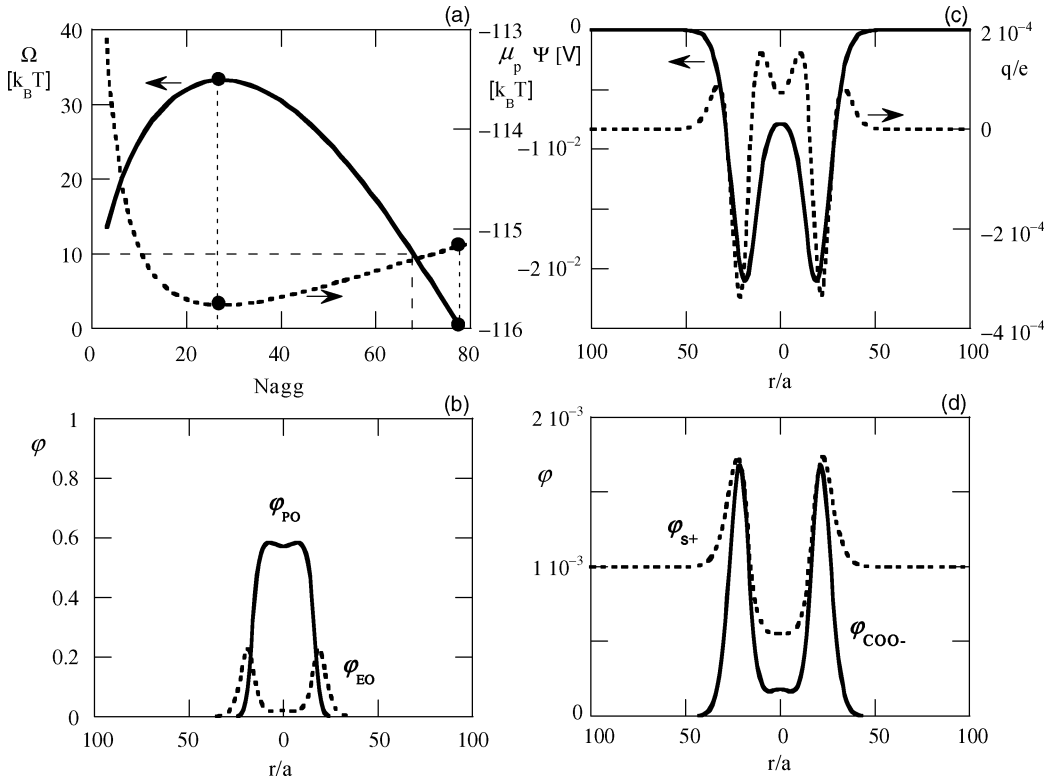

Figure 2. (a) Plot of the translationally restricted grand potential Ω (left coordinate) and chemical potential of copolymers μ_p (right coordinate) as a function of aggregation number N_{agg}. The first set of dots at $N_{agg} \approx 26$ indicates the theoretical CMC, i.e., the first appearance of thermodynamically stable micelles. The second set of dots at $N_{agg} \approx 78$ corresponds to the zero grand potential value which corresponds to the last appearance of stable micelles. The system where the restricted grand potential $\Omega = 10k_BT$ is used to depict the radial volume fraction φ of EO and PO in (b), the electrostatic potential Ψ and charge density q in (c), and the radial volume fraction φ of positive salt ion φ_{s^+} and the negative carboxylic group φ_{COO^-} in (d). The radial coordinate is denoted as r in the unit of a lattice site a. All the plots are for the block copolymer CAE-85 at pH = 7 and $\varphi_s = 10^{-3}$.

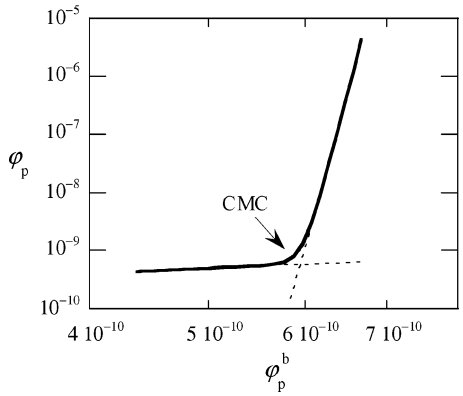

Figure 3. Total block copolymer volume fraction φ_p as a function of the bulk value φ_p^b. The curve begins at the unimeric region where there are no micelles. As the copolymer concentration increases, an abrupt change occurs which indicates the first formation of micelles. This, by definition, is CMC as indicated with the arrow. The parameters are as in Figure 2.

The plot of aggregation number N_{agg} with respect to pH at different values of electrolyte concentration $\varphi_s = 10^{-5}$ to 10^{-2} can be found in Figure 5a. In general, N_{agg} decreases with increasing pH following the increasing degree of dissociation of the carboxylic groups α_{COO^-} (cf. Figure 4b). At a higher φ_s, however, the N_{agg} decreases less dramatically due to the screening effect. In Figure 5b, the aggregation number N_{agg} is plotted as a function of φ_s for pH = 3.5, 4.5, and 5.5. For given pH, the N_{agg} increases with φ_s. Again, at pH < pK_a, the aggregation number is relatively independent of φ_s since the micelle is hardly charged and the electrostatic effect is not

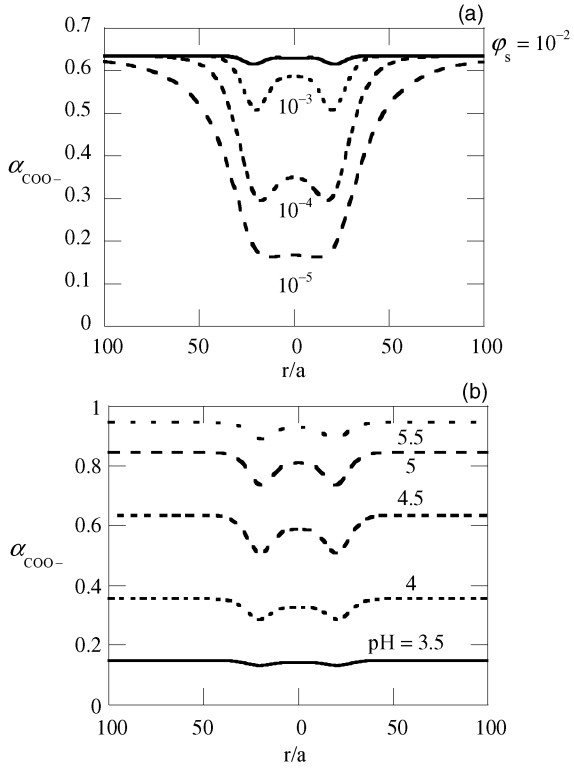

Figure 4. (a) Degree of dissociation α_{COO^-} of carboxylic groups in the copolymers CAE-85 in the radial direction r at pH = 4.5 for various values of electrolyte concentration φ_s as indicated. (b) Similar plot at $\varphi_s = 10^{-3}$ for different values of pH = 3.5, 4, 4.5, 5, and 5.5. All plots are made for micelles that have a grand potential value $\Omega = 10k_BT$.

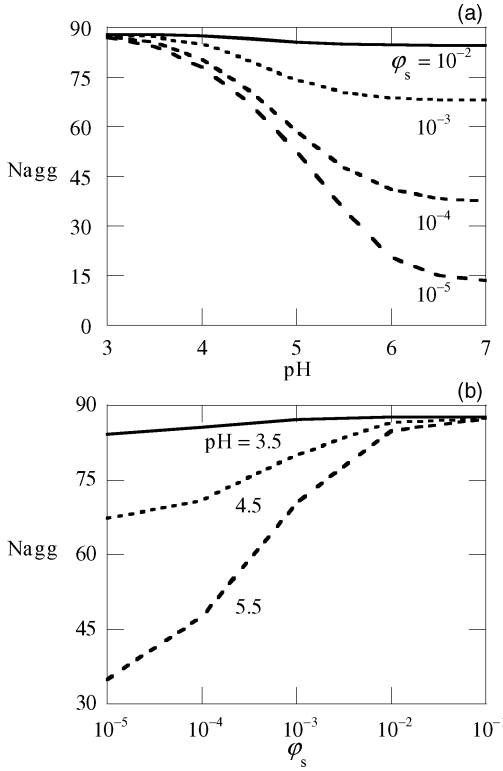

Figure 5. (a) Plot of the aggregation number N_{agg} of block copolymers CAE-85 as a function of pH for different value of electrolyte concentration, i.e., $\varphi_s = 10^{-2}$, 10^{-3}, 10^{-4}, and 10^{-5}. (b) Similar plot of the N_{agg} vs φ_s at pH = 3.5, 4.5, and 5.5 as indicated. All plots are made at the restricted grand potential value $\Omega = 10k_BT$.

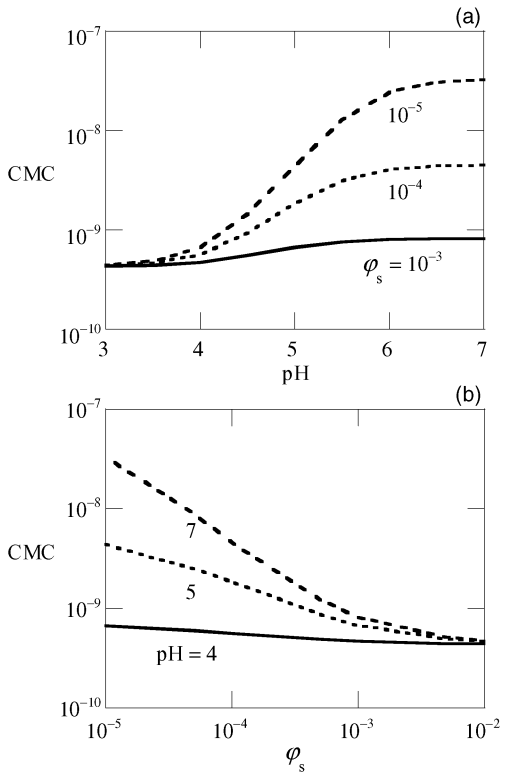

Figure 6. (a) Plot of the theoretical CMC of block copolymers CAE-85 as a function of pH for different value of electrolyte concentration, i.e., $\varphi_s = 10^{-3}$, 10^{-4}, and 10^{-5} as indicated. (b) Similar plot of the CMC vs φ_s at pH = 4, 5, and 7 as indicated.

operational (cf. Figure 4 b). At pH $\geq$ pK_a, the effect of changing electrolyte concentration is more prominent because of the combination of screening effect and the significant dependence of the degree of dissociation α_{COO^-} on φ_s as already shown in Figure 4a.

The trends of the CMC with respect to pH and φ_s variation are opposite to the trends in the aggregation number N_{agg}. The plots of the theoretical CMC, which is the volume fraction φ_p^b of CAE-85 in the bulk solution at the maximum value of the $\Omega(N_{agg})$, are depicted in Figure 6a as a function of the pH at $\varphi_s = 10^{-5}$ to 10^{-3}. The CMC increases with pH which is most dramatic at low φ_s. In Figure 6b, the CMC is plotted as a function of φ_s at different pH = 4, 5, and 7. As φ_s increases, the CMC decreases. As expected, this decrease is more significant at high pH. Nevertheless, at relatively high φ_s, in this case at about $\varphi_s = 10^{-2}$, the CMC reaches a common (fully screened) value as shown in the figure.

As mentioned above in the case study, a spherical micelle that is formed by block copolymers consists of two distinct regions, i.e., the core which mainly consists of the hydrophobic block and the corona where the hydrophilic part is mostly located. The radius of the core is denoted by R_{core} and the corona thickness by T_{corona}. In this article, the R_{core} and the T_{corona} of a micelle that consists of the CAE-85 and CAC-85 block copolymers are obtained from the density profile of PO and EO groups, respectively. The first moment of each group with respect to the center of the micelle indicates the size of the core or the corona region. Since the radial profile of PO groups resembles a step function, thus the R_{core} is defined as twice the first moment of the PO groups from the center of the micelle. The Gaussian-like radial profile of EO groups leads to the definition of T_{corona}, which is defined as the first moment of the EO groups from the center of the micelle minus the R_{core}.

The dependences of these size characteristics with pH and φ_s can be found in Figure 7. The pH-induced changes of R_{core} and T_{corona} at fixed $\varphi_s = 10^{-5}$ are given in Figure 7a. In this figure, it is shown that the R_{core} decreases at increasing pH which is directly linked to the decrease in N_{agg} (cf. Figure 5a). The thickness of the corona T_{corona} depends weakly on the pH. This is due to a compensating effect between the decrease in N_{agg} and the increasing repulsion between charged groups. These repulsions stretch the corona regardless the fact that the carboxylic groups are located in the outskirts of the corona region, i.e., at corona−solution interface. The T_{corona} increases with pH until about pH = 5.5 and decreases slightly at pH > 5.5 since in this pH region the carboxylic groups are fully charged (cf. Figure 4b).

In Figure 7b, the R_{core} and T_{corona} are plotted as a function of φ_s at fixed pH = 4.5. Again, R_{core} increases with φ_s following the increasing N_{agg} (cf. Figure 5b) and the T_{corona} decreases weakly at increasing φ_s due to the compensating effect between the increase in N_{agg} that induces a larger corona and the screening of the electrostatic potential that suppresses the corona.

The variation of R_{core} vs pH at different $\varphi_s = 10^{-5}$ to 10^{-1} is depicted in Figure 7c. The behavior of R_{core} is analogous to N_{agg} (Figure 5a). A similar plot showing the dependence of T_{corona} on the pH is depicted in Figure 7d. In general, the T_{corona} increases with pH at all indicated electrolyte concentrations except at $\varphi_s = 10^{-5}$. At pH > 5.5, the T_{corona} decreases with increasing pH since it is apparent that the severe decrease of N_{agg} at this pH range (cf. Figure 5a) overcompensates the repulsion between the charged groups.

C. Temperature Variations. As already explained in the model parameters section, the temperature-dependent behavior

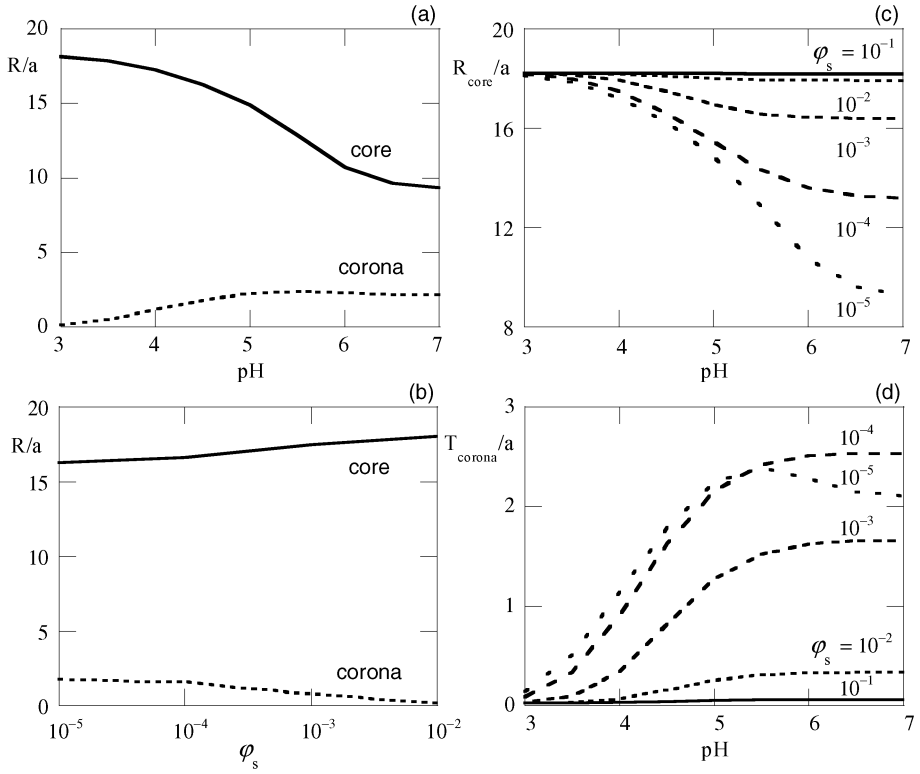

Figure 7. (a) Plot of radius of the core R_{core} and corona thickness T_{corona} of a micelle composed of CAE-85 copolymers at $\varphi_s = 10^{-5}$ for various pH. (b) Similar plot of R_{core} and T_{corona} at pH = 4.5 as a function of φ_s. (c) Plot of R_{core} vs pH at $\varphi_s = 10^{-5}$ to 10^{-1}. (d) Plot of T_{corona} vs pH at $\varphi_s = 10^{-5}$ to 10^{-1}. Each size is the distance from the center of the micelle and in the unit of the characteristic lattice site a and all plots are for micelles with a grand potential value $\Omega = 10k_BT$.

of modified Pluronics is implemented by changing the Flory−Huggins χ parameter between oxygen and water segments, i.e., χ_{OW}. It is assumed that χ_{OW} is proportional to the inverse of temperature such that the increase of the temperature causes a decrease in χ_{OW}, i.e., a decrease of the attractive interactions between these two entities. It is clear that the grand potential as a function of aggregation number $\Omega(N_{agg})$ strongly depends on χ_{OW}. Within this Ansatz, the CMT is defined by the value of χ_{OW} for which the maximum value of the restricted grand potential Ω_{max} is equal to a certain value for which, quite arbitrarily, the value $10k_BT$ is chosen. The cloud point temperature CPT is related to the specific χ_{OW} value for which the stable micellar region does no longer occur.

The dependences of the CMC and the N_{agg} with temperature (χ_{OW}) for different electrolyte concentration φ_s and pH values are shown in Figure 8. Here, the micelle is composed of CAE-85 block copolymers with varying value of $\varphi_s = 10^{-5}$ to 10^{-3} at pH = 7 (Figure 8a,c) and pH = 4, 5, and 7 at $\varphi_s = 10^{-4}$ (Figure 8b,d) with χ_{OW} ranges from − 0.9 to −0.6. It is known that the increase of χ_{OW}, i.e., the increase of temperature, leads to the decrease of CMC. This is shown in Figure 8a,c for all indicated φ_s and pH variations, for which all CMC values decrease in almost the same way. Correspondingly, the N_{agg} increases with rising temperature (less negative χ_{OW}) for all pH and electrolyte concentration values that are used (Figure 8b,d).

In parts a and b of Figure 9, the χ_{OW} values corresponding to the CMT and the CPT are depicted as a function of $\varphi_s = 10^{-5}-10^{-2}$ at pH = 5 and 7, respectively. It can be seen that the CMT and CPT decrease when φ_s increases and the decrease is more siginificant at higher pH values. At sufficiently high φ_s values, the electrostatic potential of the charged micelle is effectively screened such that the corresponding CMT or CPT reach a limiting value.

D. CAE-85 vs CAC-85. As already mentioned in the Introduction, our interest is in two types of block copolymers. They differ on the location of the carboxylic groups with respect to the original configuration of PEO and PPO entities in the Pluronic, i.e., in the end of PEO chains (CAE-85) and between PEO and PPO blocks (CAC-85). The differences in micellization properties for both type of block copolymers are discussed below.

In Figure 10a, the N_{agg} of a micelle either from block copolymers CAE-85 or CAC-85 at $\varphi_s = 10^{-4}$ are plotted with respect to pH. For both types of block copolymers, the N_{agg} decreases at increasing pH. A more dramatic decrease is found for the micelle from block copolymers CAC-85. The location of carboxylic group between hydrophilic EO and hydrophobic PO groups (at core−corona interface) makes the micelle more sensitive to an increase of the total number of charges (as the pH increases). In Figure 10b, the aggregation number N_{agg} for both types of block copolymers are plotted as a function of φ_s at fixed pH = 7. As discussed above, the N_{agg} increases with φ_s due to screening effect of the electrostatic potential. A more dramatic change of N_{agg} happens for the micelle composed of block copolymers CAE-85. This may be due to an easier accumulation of counterions at the corona−solution interface since the counterions do not need to penetrate completely to the hydrophobic core region.

The variation of CMC composed of either CAE-85 or CAC-85 block copolymers, with respect to varying pH at fixed $\varphi_s = 10^{-4}$, varying φ_s at fixed pH = 7 and varying χ_{OW} at $\varphi_s = 10^{-4}$ and pH = 7 can be found in parts a, b, and c of Figure 11, respectively. Obviously, the same trend of CMC is found for both types of applied block copolymers. The CMC increases with pH and decreases for each case with increasing φ_s and

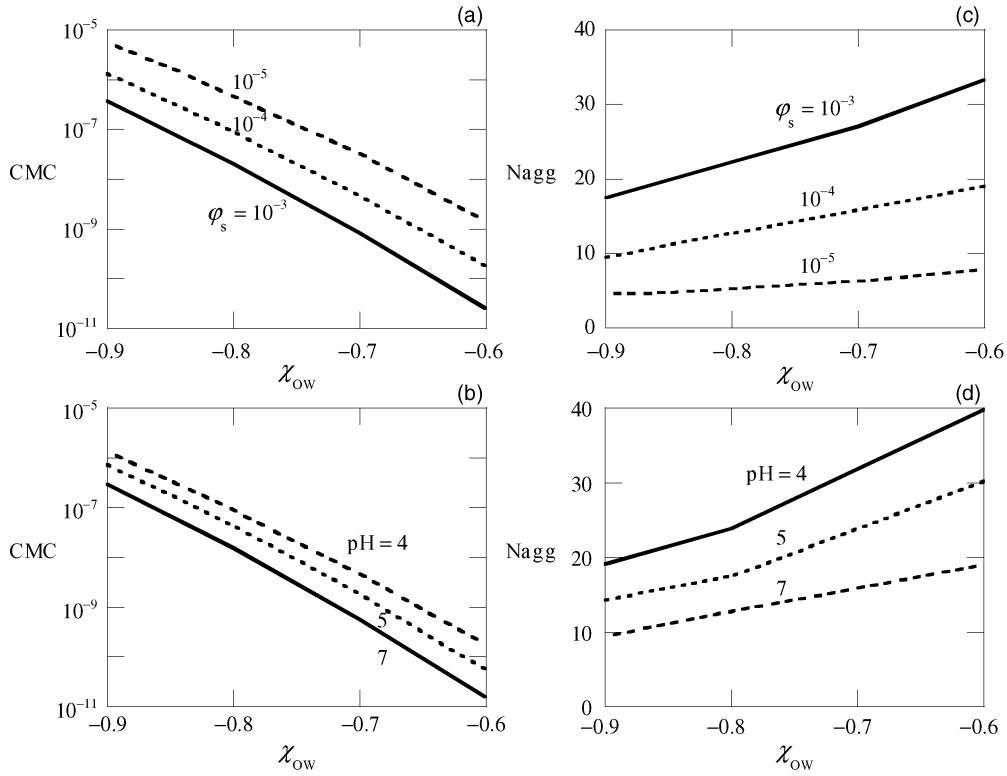

Figure 8. (a) Plot of theoretical CMC of block copolymers CAE-85 as a function of χ_{OW} at pH = 7 for different value of electrolyte concentration, i.e., $\varphi_s = 10^{-3}$, 10^{-4}, and 10^{-5}, as indicated. (b) Similar plot of CMC vs χ_{OW} at $\varphi_s = 10^{-4}$ for different values of pH = 4, 5, and 7, as indicated. (c) Plot of corresponding N_{agg} at the CMC as a function of χ_{OW} at pH = 7 for different value of $\varphi_s = 10^{-3}$, 10^{-4}, and 10^{-5}. (d) Similar plot of N_{agg} at the CMC vs χ_{OW} at $\varphi_s = 10^{-4}$ for different value of pH = 4, 5, and 7.

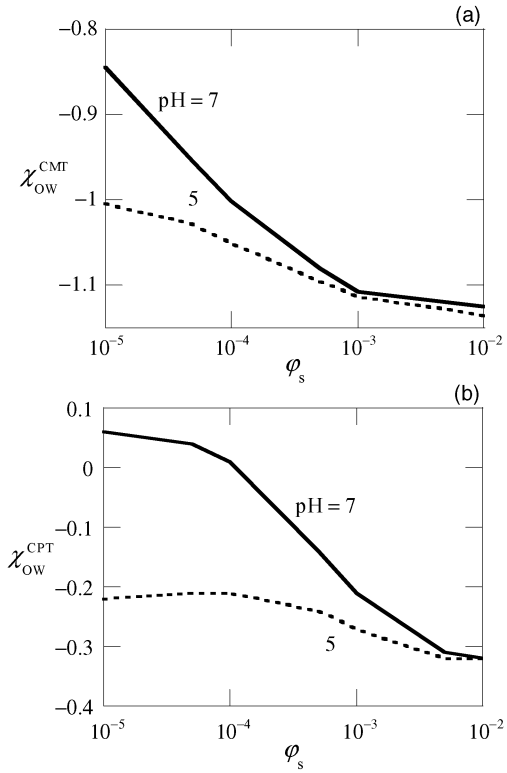

Figure 9. (a) The interaction parameter χ_{OW}^{CMT}, that corresponds directly to CMT, as a function of φ_s at pH = 5 and 7, as indicated. (b) The corresponding CPT as a function of φ_s at pH = 5 and 7. The micelle is composed of CAE-85 block copolymers.

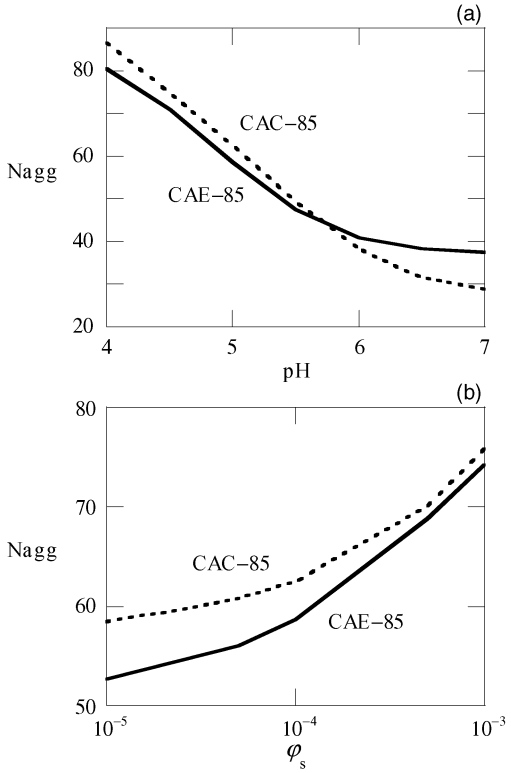

Figure 10. (a) Plot of the aggregation number N_{agg} of a micelle from block copolymers CAE-85 or CAC-85, with respect to pH at $\varphi_s = 10^{-4}$. (b) Similar plot of the aggregation number N_{agg} as a function of φ_s at pH = 5. All plots are made for micelles with the restricted grand potential value $\Omega = 10k_BT$.

temperature. However, in all variations, the micelle from CAC-85 block copolymers has higher CMC values than for the case of CAE-85.

The CMT (Figure 12a) follows the behavior of CMC with increasing φ_s (Figure 11b); i.e., there is a decrease of CMT

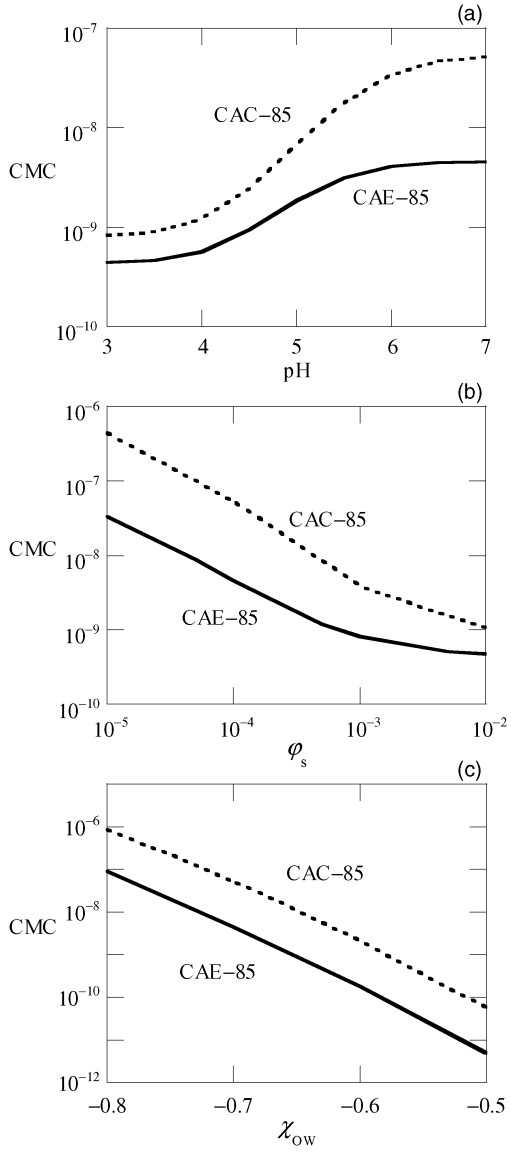

Figure 11. (a) The CMC of a micelle composed of CAE-85 or CAC-85 block copolymers as a function of the pH at $\varphi_s = 10^{-4}$. (b) Similar plot of the CMC as a function of φ_s at pH = 7. (c) Similar plot of the CMC as a function of χ_{OW} at $\varphi_s = 10^{-4}$ and pH = 7.

with increasing φ_s. The CPT also decreases upon increasing φ_s as can be seen in Figure 12b. However, the CPT for the micelle composed of block copolymers CAE-85 is higher than it of the CAC-85. This means that the phase separation happens at lower temperature for this type of block copolymer.

VI. Conclusion and Remarks

The micellization properties of modified Pluronic block copolymers CAE-85 and CAC-85 are investigated by means of self-consistent-field approximation. As a result of the presence of the carboxylic groups in the block copolymers, the micellization depends on the pH and added electrolyte concentration φ_s, as well as the temperature. The dependencies of the aggregation number N_{agg}, micellar size, and CMC, with respect to three governing parameters: pH, φ_s, and temperature, are studied, where the influence of the temperature is mimicked by the change of the Flory−Huggins interaction parameter χ_{OW}.

From the calculation, it is shown that as the pH increases the N_{agg} and, consequently, the core radius, R_{core}, decrease. However, the CMC increases with increasing pH, and except

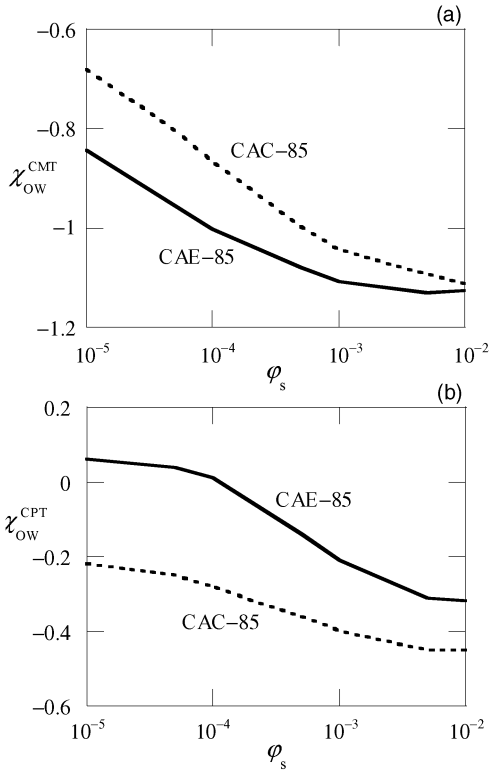

Figure 12. (a) The interaction parameter χ_{OW}^{CMT} that corresponds to the χ_{OW} at the CMT. It is depicted as a function of φ_s for a micelle which is composed of either CAE-85 or CAC-85 block copolymers, as indicated. (b) Similar plot for corresponding χ_{OW}^{CPT} as a function of φ_s.

for very low φ_s, the corona thickness T_{corona} also increases with pH. Furthermore, the N_{agg} and R_{core} increase with φ_s while the CMC and T_{corona} decrease at increasing φ_s. At low φ_s, the CMT and CPT increase with pH and the decreasing trend is found for CMT and CPT as φ_s increases.

Interestingly, the position of carboxylic groups in the micelle is important for, e.g., the CMT or CPT. This is significant for the applications of temperature-sensitive ionic micelles. One possible application is the metal binding capacity of these micelles. The modeling of this aspect is the target of current investigations.

Acknowledgment. The Dutch Science and Technology Foundation (STW), Aquacare, GWA, KIWA, Witteveen&Bos and ETD&C are greatly acknowledged for financial support (Grant EPC.5516).

References and Notes

(1) Alexandridis, P.; Holzwarth, J. F.; Hatton, T. A. *Macromolecules* **1994**, *27*, 2414−2425.
(2) Alexandridis, P.; Hatton, T. A. *Colloids Surf., A* **1995**, *96*, 1−46.
(3) Brown, W.; Schillen, K.; Almgren, M.; Hvidt, S.; Bahadur, P. *J. Phys. Chem.* **1991**, *95*, 1850−1858.
(4) Glatter, O.; Scherf, G.; Schillen, K.; Brown, W. *Macromolecules* **1994**, *27*, 6046−6054.
(5) Michels, B.; Waton, G.; Zana, R. *Langmuir* **1997**, *13*, 3111−3118.
(6) Mortensen, K.; Pedersen, J. S. *Macromolecules* **1993**, *26*, 805−812.
(7) Mortensen, K.; Brown, W.; Jorgensen, E. *Macromolecules* **1994**, *27*, 5654−5666.
(8) Noolandi, J.; Shi, A. C.; Linse, P. *Macromolecules* **1996**, *29*, 5907−5919.
(9) Wanka, G.; Hoffmann, H.; Ulbricht, W. *Colloid Polym. Sci.* **1990**, *268*, 101−117.
(10) Wanka, G.; Hoffmann, H.; Ulbricht, W. *Macromolecules* **1994**, *27*, 4145−4159.
(11) Linse, P. *Macromolecules* **1993**, *26*, 4437−4449.

(12) Zhou, Z.; Chu, B. *Macromolecules* **1988**, *21*, 2548−2554.
(13) Tanford, C. *The Hydrophobic Effect*: *Formation of Micelles and Biological Membranes*; J. Wiley & Sons: New York, 1973.
(14) Privalov, P. L.; Gill, S. J. *Pure Appl. Chem.* **1989**, *61*, 1097−1104.
(15) Linse, P.; Malmsten, M. *Macromolecules* **1992**, 25, 5434−5439.
(16) Bahadur, P.; Pandya, K.; Almgren, M.; Li, P.; Stilbs, P. *Colloid Polym. Sci.* **1993**, 271, 657−667.
(17) Alexandridis, P.; Nivaggioli, T.; Hatton, T. A. *Langmuir* **1995**, 11, 1468−1476.
(18) Mortensen, K. *Europhys. Lett.* **1992**, *19*, 7, 599−604.
(19) Jorgensen, E. B.; Hvidt, S.; Brown, W.; Schillen, K. *Macromolecules* **1997**, *30*, 2355−2364.
(20) Armstrong, J. K.; Chowdhry, B. Z.; Snowden, M. J.; Leharne, S. A. *Langmuir* **1998**, *14*, 2004−2010.
(21) Pandit, N.; Trygstad, T.; Croy, S.; Bohorquez, M.; Koch, C. *J. Colloid Interface Sci.* **2000**, *222*, 213−220.
(22) Mao, G.; Sukumaran, S.; Beaucage, G.; Saboungi, M. L.; Thiyagarajan, P. *Macromolecules* **2001**, *34*, 552−558.
(23) Su, Y. L.; Liu, H. Z.; Wang, J.; Chen, J. Y. *Langmuir* **2002**, *18*, 865−871.
(24) Su, Y. L.; Wei, X. F.; Liu, H. Z. *J. Colloid Interface Sci.* **2003**, *264*, 526−531.
(25) Custers, J. P. A.; Kelemen, P.; Van den Broeke, L. J. P.; Cohen Stuart, M. A.; Keurentjes, J. T. F. *J. Am. Chem. Soc.* **2005**, *127*, 1594−1595.
(26) Israelachvili, J. N.; Mitchell, D. J.; Ninham, B. W. *J. Chem. Soc., Faraday Trans. 2* **1976**, *72*, 1525−1568.
(27) Scheutjens, J. M. H. M.; Fleer, G. J. *J. Phys. Chem.* **1979**, *83*, 1619−1635.
(28) Scheutjens, J. M. H. M.; Fleer, G. J. *J. Phys. Chem.* **1980**, *84*,. 178−190.
(29) Hurter, P. N.; Scheutjens, J. M. H. M.; Hatton, T. A. *Macromolecules* **1993**, *26*, 5592−5601.
(30) Bohmer, M. R.; Evers, O. A.; Scheutjens, J. M. H. M. *Macromolecules* **1990**, *23*, 2288−2301.
(31) Bohmer, M. R.; Koopal, L. K. *Langmuir* **1992**, *8*, 1594−1602.
(32) Hill, T. L. *Thermodynamics of Small Systems, Parts 1 and 2*; Dover Pub., Inc.: New York, 1994.
(33) Hall, D. G.; Pethica, B. A. In *Nonionic Surfactants*; Schick, M. J., Ed.; Marcel Dekker, Inc.: New York, 1967; Chapter 16.
(34) Gibbs, J. W. *The scientific papers of J. Willard Gibbs, Vol. 1*: *Thermodynamics*; Ox Bow Press: Woodbridge, 1993.
(35) Bjorling, M.; Linse, P.; Karlstrom, G. *J. Phys. Chem.* **1990**, *94*, 471−481.
(36) Israels, R. Adsorption of Charged Diblock Copolymers: Effect on Colloidal Stability. Doctoral Thesis, Wageningen, 1994.
(37) Van Male, J. Self-Consistent-Field Theory for Chain Molecules: Extensions, Computational Aspects, and Applications. Doctoral Thesis, Wageningen, 2003.
(38) Israels, R.; Leermakers, F. A. M.; Fleer, G. J. *Macromolecules* **1994**, *27*, 3087−3093.
(39) Van der Vegte, E. W.; Hadziioannou, G. *J. Phys. Chem. B* **1997**, *101*, 9563−9569.
(40) Kokkoli, E.; Zukoski, C. F. *Langmuir* **2000**, *16*, 6029−6036.
(41) Van der Schoot, P. P. A. M.; Leermakers, F. A. M. *Macromolecules* **1988**, *21*, 1876−1877.
(42) Evers, O. A.; Scheutjens, J. M. H. M.; Fleer, G. J. *Macromolecules* **1990**, *23*, 5221−5233.
(43) Oversteegen, S. M.; Leermakers, F. A. M. *Phys. Rev. E* **2000**, *62*, 8453−8461.
(44) De Bruijn, V. G.; Van den Broeke, L. J. P.; Leermakers F. A. M.; Keurentjes J. T. F. *Langmuir* **2002**, *18*, 10467−10474.
(45) Van der Vegte, E. W.; Hadziioannou, G. *J. Phys. Chem. B* **1997**, *101*, 9563−9569.